Widely Linear Blind Adaptive Equalization for Transmitter IQ-Imbalance/Skew Compensation in Multicarrier Systems

Edson Porto da Silva
Universidade Federal de Campina Grande (UFCG)

D. Zibar
Technical University of Denmark

Widely Linear Blind Adaptive Equalization for Transmitter IQ-Imbalance/Skew Compensation in Multicarrier Systems

Edson Porto da Silva [(1)], Darko Zibar [(1)].

[(1)] Department of Photonics Engineering, Technical University of Denmark - DTU, edpod@fotonik.dtu.dk.

Abstract *Simple analytical widely linear complex-valued models for IQ-imbalance and IQ-skew effects in multicarrier transmitters are presented. To compensate for such effects, a 4×4 MIMO widely linear adaptive equalizer is proposed and experimentally validated.*

Introduction

The use of baud rate optimized multicarrier systems has recently been proposed as a robust approach to mitigate the impact of fiber nonlinear interference (NLI)[1,2]. However, the performance of such systems can be degraded by imperfections or improper calibration at the transmitters or receivers that can lead to IQ-imbalance and IQ-skew[3], here generally referred to as IQ-mixing effects. In presence of any of these effects, it can be shown that the set of generated subcarriers will suffer from linear self interference[4]. Recently, a least mean square (LMS) 8×8 multiple-input multiple output (MIMO) real adaptive equalizer has been proposed to compensate for IQ-skew present at the subcarrier transmitter[4]. However, the LMS algorithm requires knowledge of the phase of all subcarriers at the receiver simultaneously, which can be a difficult task before polarization demultiplexing and equalization.

As alternative solution, a blind equalization strategy can be employed[5,6]. Blind equalization algorithms usually rely on the two-dimensional statistical properties of the signals described in the complex domain. However, IQ-mixing interference can not be completely captured by *standard* (strictly) linear models in the complex domain[7], commonly used for adaptive equalization in polarization multiplexed systems. Therefore, in order to make the equalization robust to such effects, the usual complex-valued equalizer models have to be extended to include IQ-mixing.

The novel contributions of this paper are: 1) a simple analytical widely linear (WL) complex-valued model to describe the impact of IQ-mixing effects in multicarrier transmitters is proposed; 2) based on the analytical model, a new WL 4×4 MIMO complex-valued adaptive equalizer is proposed for compensating IQ-mixing effects originating from multicarrier transmitters. The equalizer is experimentally validated for a multicarrier system with four 8 GBd Nyquist DP-QPSK subcarriers.

Widely Linear Complex-valued Models for IQ-Mixing Effects in Multicarrier Transmitters

Consider a system with an even number N_{sc} of subcarriers, for simplicity, uniformly separated in frequency by f_{sc} Hz. The complex baseband envelope of the entire set of subcarriers is given by

$$s(t) = \sum_{k=1}^{N_{sc}} s_k(t) \exp\left[\frac{-j\alpha(k)\omega_{sc}t}{2}\right] \tag{1}$$

where $s_k(t)$ is the complex baseband signal corresponding to the individual subcarrier of index k, $\omega_{sc} = 2\pi f_{sc}$ and $\alpha(k) = 2k - 1 - N_{sc}$. The index $k = 1$ refers to the subcarrier in the *left* most position in the spectrum. The conjugate version of $s(t)$ is given by

$$s^*(t) = \sum_{n=1}^{N_{sc}} s_n^*(t) \exp\left[\frac{-j\beta(n)\omega_{sc}t}{2}\right] \tag{2}$$

where $\beta(n) = -2n + 1 + N_{sc}$. Observe that $n = 1$ corresponds to the conjugate subcarrier in the *right* most position of the spectrum.

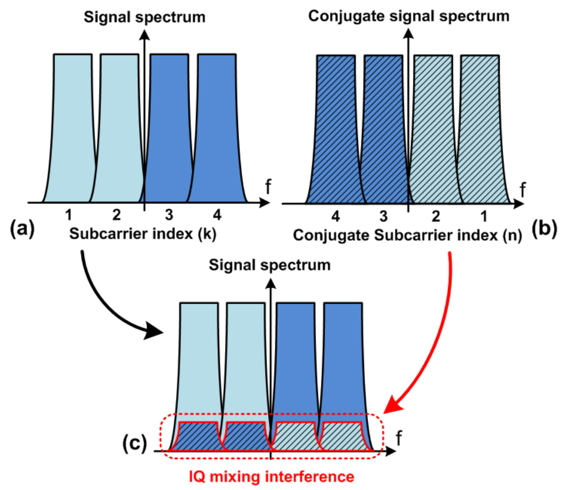

Figure 1 Illustration of IQ-mixing interference effect for a multicarrier system with four subcarriers.

The effect of IQ-imbalance can be described by the WL transformation in the complex domain

$$\hat{s}(t) = k_1 s(t) + k_2 s^*(t) \Rightarrow \hat{S}(\omega) = k_1 S(\omega) + k_2 S^*(-\omega) \tag{3}$$

where k_1 and k_2 are complex numbers[8], and $S(\omega)$ is the Fourier transform of $s(t)$. Moreover, IQ-skew can also be modeled by a WL transformation of $s(t)$, represented in the frequency domain by

$$\hat{S}(\omega) = G_1(\omega)S(\omega) + G_2(\omega)S^*(-\omega) \tag{4}$$

where $G_1(\omega) = \cos(\omega\tau/2)$ and $G_2(\omega) = j\sin(\omega\tau/2)$, with τ corresponding to the skew value in seconds.

Therefore, if the subcarrier transmitter suffers

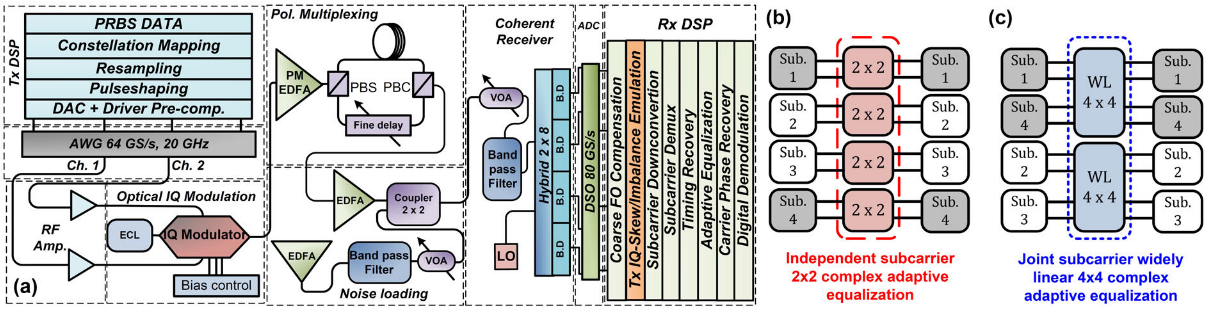

Figure 2 (a) Experimental setup to generate and coherently detect a 4×8 Gbaud DP-QPSK Nyquist multicarrier signal and offline DSP applied to the traces. (b) The individual subcarrier equalization scheme using 2×2 MIMO complex-valued adaptive equalizer. (c) The proposed equalization scheme using 4×4 MIMO WL complex-valued adaptive equalizer.

from IQ-mixing, the equivalent complex baseband signal $\hat{s}(t)$ will be the result of linear self interference between $s(t)$ and its conjugate. This implies that each subcarrier $\hat{k}$ will receive linear crosstalk from the *conjugate version* of a subcarrier $\hat{n}$. The pairs of interfering subcarriers can be determined using Eq. (1) and Eq. (2), under the condition $\alpha(\hat{k}) = \beta(\hat{n})$. Therefore, interfering subcarriers obey the relation $\hat{k}+\hat{n} = N_{sc}+1$. For example, for a system with 4 subcarriers, the interfering pairs are (1, 4) and (2, 3), as illustrated in Fig. 1.

The proposed model describes either the IQ-mixing happening *only* at the transmitter or *only* at the receiver front end in a back-to-back configuration. Here we assume that *only* the transmitter imposes IQ-mixing to the signals because, in this case, the model holds also if the signal is detected after propagation over the fiber channel. However, if IQ-mixing is induced at the receiver front end after fiber propagation, the model has to be modified to account for the chromatic dispersion and this case is not investigated here.

4×4 MIMO Widely Linear Complex-valued Adaptive Equalizer Structure

Based on the models in the previous section we propose a MIMO WL complex-valued adaptive equalizer structure able to compensate the IQ-mixing interference from dual polarization multicarrier transmitters. The finite impulse response (FIR) structure of the equalizer is given by

$$\begin{bmatrix}\hat{x}_A\\ \hat{y}_A\end{bmatrix}=\begin{bmatrix}\boldsymbol{h}^H_{\mathrm{x_A x_A}} & \boldsymbol{h}^H_{\mathrm{x_A y_A}}\\ \boldsymbol{h}^H_{\mathrm{y_A x_A}} & \boldsymbol{h}^H_{\mathrm{y_A y_A}}\end{bmatrix}\begin{bmatrix}\boldsymbol{x}_A\\ \boldsymbol{y}_A\end{bmatrix}+\begin{bmatrix}\boldsymbol{h}^H_{\mathrm{x_A x_B^*}} & \boldsymbol{h}^H_{\mathrm{x_A y_B^*}}\\ \boldsymbol{h}^H_{\mathrm{y_A x_B^*}} & \boldsymbol{h}^H_{\mathrm{y_A y_B^*}}\end{bmatrix}\begin{bmatrix}\boldsymbol{x}_B^*\\ \boldsymbol{y}_B^*\end{bmatrix}$$

$$\begin{bmatrix}\hat{x}_B\\ \hat{y}_B\end{bmatrix}=\begin{bmatrix}\boldsymbol{h}^H_{\mathrm{x_B x_B}} & \boldsymbol{h}^H_{\mathrm{x_B y_B}}\\ \boldsymbol{h}^H_{\mathrm{y_B x_B}} & \boldsymbol{h}^H_{\mathrm{y_B y_B}}\end{bmatrix}\begin{bmatrix}\boldsymbol{x}_B\\ \boldsymbol{y}_B\end{bmatrix}+\begin{bmatrix}\boldsymbol{h}^H_{\mathrm{x_B x_A^*}} & \boldsymbol{h}^H_{\mathrm{x_B y_A^*}}\\ \boldsymbol{h}^H_{\mathrm{y_B x_A^*}} & \boldsymbol{h}^H_{\mathrm{y_B y_A^*}}\end{bmatrix}\begin{bmatrix}\boldsymbol{x}_A^*\\ \boldsymbol{y}_A^*\end{bmatrix} \tag{5}$$

where $(\boldsymbol{x}, \boldsymbol{y})$ correspond to the signals from distinct polarization, and the indexes $(A,\ B)$ indicate any pair of interfering subcarriers defined in the previous section. All vectors $\boldsymbol{h}$, $\boldsymbol{x}_A$, $\boldsymbol{y}_A$, $\boldsymbol{x}_B$, $\boldsymbol{y}_B \in \mathbb{C}^{N\times 1}$, where N is the number of FIR taps. The error criteria can be selected according the type of training intended. For proof of concept with QPSK subcarriers, blind training is assumed using the constant modulus algorithm (CMA) and a $T/2$-fractionally spaced structure (2 samples/symbol). The experimental validation of the proposed complex-valued equalizer is then reported in the next sections.

Experimental setup

The experimental setup is shown in Fig. 2 (a). At the transmitter side, an in-phase and quadrature (IQ) modulator is used to modulate one external cavity laser (ECL), with linewidth less than 100 kHz. The signals used to drive the optical IQ modulator are provided by an arbitrary waveform generator (AWG) with a sample-rate of 64 GSa/s and an analog bandwidth of 20 GHz. The modulated baseband signal synthesized by the AWG is composed by four decorrelated QPSK carriers, each modulated at 8 GBd, with root raised cosine (RRC) pulse shape with a roll-off factor of 1%, and separated by 500 MHz guard bands. The data of all QPSK subcarriers are generated by a pseudo random bit sequence (PRBS, $2^{23}-1$). The optical signal is amplified and sent to a polarization multiplexing emulation stage, in order to get the final DP-QPSK desired multicarrier set. After noise loading, the signal is pre-amplified, filtered, and coherently detected with a single optical coherent receiver. The detected signal is acquired with a real time digital sampling oscilloscope (DSO) at 80 GSa/s and 33 GHz of analog bandwidth. Offline digital signal processing (DSP) is used to process the acquired data. The flow of algorithms is composed of coarse frequency offset (FO) compensation, subcarrier demultiplexing (downconversion and matched filtering), timing recovery, adaptive equalization, carrier phase recovery, digital demodulation and bit error counting.

Since in the experimental setup it was not possible to set a large and precise range of IQ-skew and IQ-imbalance values at the transmitter side, those effects were emulated offline to the detected data. Nevertheless, as the experimental analysis is restricted to the back-to-back case, the proposed model holds. To add a specific skew value, IQ components of the acquired polarizations were shifted in time by a corresponding number of samples. Phase and amplitude

IQ-imbalance are added to the signals based on models provided in reference [8]. The performance was investigated for a total of 121 combinations of IQ-skew and 441 of IQ-imbalance.

Results

In the following analysis, the performance of the system using a dual-subcarrier 4×4 MIMO WL complex-valued adaptive equalizer (Fig. 2(c)) is compared against the case where each of the four subcarriers is independently equalized by a 2×2 MIMO complex-valued adaptive equalizer (Fig. 2(b)). In both equalizers, CMA is used as adaptation rule for 41-taps FIR coefficients. The Q^2-factor is calculated from the average bit error rate (BER) of the multicarrier set after convergence of the equalizers in the mean square error (MSE) sense. For all cases, the OSNR (0.1 nm bandwidth) at the receiver input was fixed at 21 dB, which resulted in a average BER of 2×10^{-4} (Q^2-factor of $\approx$ 11 dB) for the multicarrier signal in absence of any IQ-mixing effects. The BER is calculated over more than 1.2×10^6 bits.

Figures 4 and 3 show the Q^2-factor surfaces obtained w.r.t IQ amplitude imbalance and IQ phase imbalance, respectively.

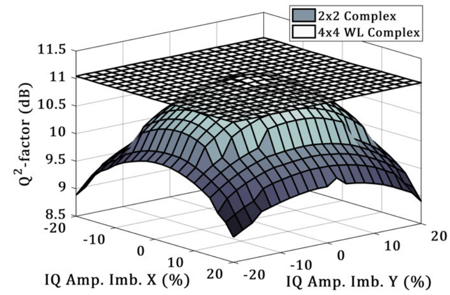

Figure 3 Average Q^2-factor of all subcarriers versus the percentage of IQ amplitude imbalance of each polarization.

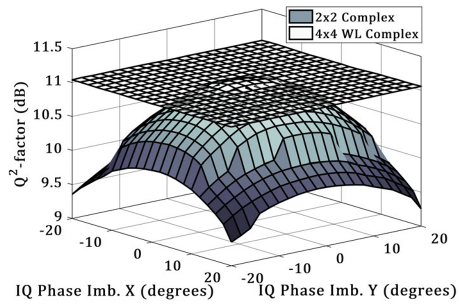

Figure 4 Average Q^2-factor of all subcarriers versus IQ phase imbalance in each polarization.

For all investigated combinations, the same performance is obtained with the 4×4 WL equalizer. On the other hand, because the interference from the conjugate subcarriers can not be compensated, a performance penalty appears for the case where each subcarrier is individually processed by a 2×2 equalizer. The performance of both equalizers is virtually the same in absence of IQ-imbalance. Figure 5 shows the Q^2-factor surfaces obtained for up to a half-symbol of IQ-skew in each polarization.

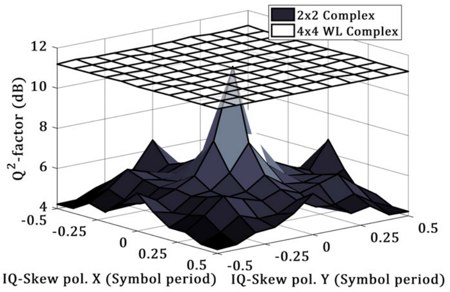

Figure 5 Average Q^2-factor of all subcarriers versus IQ-skew as a fraction of the symbol period in each polarization.

It can be noted that the penalty induced by IQ-skew is much higher that the penalty from IQ-imbalance for the 2×2 equalizer case. This can be attributed to the frequency dependence of Eq. (4). However, even for a half-symbol IQ-skew, no penalty is observed with the 4×4 WL equalizer. The performance of both equalizers is virtually the same in absence of IQ-skew.

Conclusions

Experimental results show that the proposed widely linear complex-valued equalizer is able to maintain the multicarrier system performance over broad range of transmitter IQ-imbalance and IQ-skew combinations. The results also validate the proposed complex-valued models for IQ-mixing effects in multicarrier transmitters.

Acknowledgements

This work was supported by VILLUM FOUNDATION and the DNRF Research Centre of Excellence.

References

[1] M. Qiu *et al.*, "Digital subcarrier multiplexing for fiber nonlinearity mitigation in coherent optical communication systems," Opt. Express, vol. 22, no. 15, p. 18770 (2014)

[2] A. Nespola *et al.*, "Experimental demonstration of fiber nonlinearity mitigation in a WDM multi-subcarrier coherent optical system," Proc. ECOC 2015, paper Mo.3.6.3 (2015)

[3] M. S. Faruk and K. Kikuchi, "Compensation for in-phase/quadrature imbalance in coherent-receiver front-end for optical quadrature amplitude modulation," IEEE Photonics J., vol. 5, no. 2 (2013).

[4] G. Bosco *et al.*, "Impact of the transmitter IQ-skew in multi-subcarrier coherent optical systems," in Proc. OFC 2016, paper W4A.5 (2016).

[5] R. Rios-Müller *et al.*, "Blind receiver skew compensation and estimation for long-haul non-dispersion managed systems using adaptive equalizer," J. Light. Technol., vol. 33, no. 7, pp. 1315 (2015).

[6] M. Paskov *et al.*, "Blind equalization of receiver in-phase/quadrature skew in the presence of Nyquist filtering," IEEE Photon. Technol. Lett., vol. 25, no. 24, pp. 2446 (2013).

[7] T. Adali *et al.*, "Complex-Valued Signal Processing: The Proper Way to Deal With Impropriety," IEEE Trans. Signal Process., vol. 59, no. 11, pp. 5101 (2011).

[8] P. Rykaczewski *et al.*, "On the connection of I/Q imbalance and channel equalization in direct-conversion transceivers," IEEE Trans. Veh. Technol., vol. 57, no. 3, pp. 1630 (2008).